Element-specific magnetic moments from core-absorption magnetic circular dichroism of the doped Heusler alloy $Co_2Cr_{0.6}Fe_{0.4}Al$

H. J. Elmers, G. H. Fecher, D. Valdaitsev, S. A. Nepijko, A. Gloskovskii, G. Jakob, and G. Schönhense
Institut für Physik, Johannes Gutenberg-Universität Mainz, D-55099 Mainz, Germany

S. Wurmehl, T. Block, and C. Felser
Institut für Anorganische Chemie und Analytische Chemie, Johannes Gutenberg-Universität Mainz, D-55099 Mainz, Germany

P.-C. Hsu and W.-L. Tsai
Institute of Physics, Academia Sinica, Nankang, Taipei 11529, Taiwan

S. Cramm
Institut für Festkörperforschung, Forschungszentrum Jülich GmbH, D-52425 Jülich, Germany
(Received 27 September 2002; revised manuscript received 15 January 2003; published 17 March 2003)

The magnetic circular dichroism (MCD) of core-level absorption (x-ray absorption spectroscopy, XAS) spectra in the soft x-ray region has been measured for the ferromagnetic Heusler alloy $Co_2Cr_{0.6}Fe_{0.4}Al$ at the Co, Fe, and Cr $L_{II,III}$ edges. The comparison of XAS spectra before and after *in situ* cleaning of polished surfaces revealed a pronounced selective oxidation of Cr in air. For clean surfaces we observed a MCD for all three elements with Fe showing the largest moment per atom. The MCD can be explained by the density of states of the $3d$ unoccupied states, predicted by linear muffin-tin orbital atomic sphere approximation. For Fe and Cr the orbital angular momentum component of the magnetic moment is considerably larger than the values reported for metallic alloys, whereas for Co a value close to its bulk value is observed. This observation is discussed in comparison with band structure calculations.

DOI: 10.1103/PhysRevB.67.104412 PACS number(s): 75.50.Cc, 71.20.Lp, 78.40.Kc

I. INTRODUCTION

Electronic devices exploiting the spin of an electron (spintronics) have attracted great scientific interest.[1] The basic element is a ferromagnetic electrode providing a spin-polarized electrical current. Materials with a complete spin-polarization would be most desirable, i.e., a metal for spin-up and a semiconductor for spin-down electrons. Such materials are called half-metallic ferromagnets[2] (HMF) and Heusler compounds have been considered potential candidates to show this property.[2] Theoretical calculations predict an energy gap for spin down electrons for the half-Heusler compound NiMnSb,[2,3] which, however, has been controversially discussed.[4,5] Similarly, a HMF-like behavior was found by Plogmann *et al.*[6] for the Cobalt-based Heusler alloy Co_2MnSn. We focus on the Heusler compound $Co_2Cr_{1-x}Fe_xAl$, which is ferromagnetic at room temperature. The largest magnetoresistance was found for the compound with an Fe concentration of $x=0.4$ (Ref. 7).

Heusler alloys belong to a group of ternary intermetallic compounds with the stoichiometric composition X_2YZ ordered in an $L2_1$-type structure, many of which are ferromagnetic.[8] A Heusler alloy consists of two different transition metals X and Y and a nonmagnetic metal or a nonmetallic element Z. The Y and Z atoms occupy two fcc sublattices with the origins at $(0,0,0)$ and $(\frac{1}{2},\frac{1}{2},\frac{1}{2})$, respectively. The X atoms are located at $(\frac{1}{4},\frac{1}{4},\frac{1}{4})$ sublattices and have a tetrahedral symmetry with four nearest Y and four nearest Z neighbors. Y and Z atoms possess a local cubic symmetry with eight nearest X neighbors. It is important to notice that this structure easily allows for atomic disorder, either by interchange of atoms or by partial occupancy. A careful preparation is necessary to obtain reproducible results.

Ferromagnetic properties of Heusler alloys have been investigated experimentally[8–13] and theoretically.[6,14] The Co-based Heusler alloys Co_2YZ are of particular interest because they show comparatively high Curie temperatures and varying magnetic moments ranging from $0.3\mu_B$ to $1.0\mu_B$ at the Co site depending on the constituents Y and Z of the Heusler alloy.[11,15,16]

For Co_2CrAl a ground-state magnetic moment of $1.55\mu_B$ per formula unit has been reported[17] and it was considered that Co atoms mainly carry the magnetic moment in this alloy, whereas the contribution of Cr and Al atoms remains negligible.[18] Recent linear muffin-tin orbital (LMTO) band structure calculations[19] reveal a HMF character of the density of states, i.e., a gap at the Fermi level in the minority band and a high density of states in the majority band. According to our calculation all constituents of the alloy should possess a magnetic moment, $0.77\mu_B$ per atom for Co, $1.63\mu_B$ per atom for Cr, and $-0.10\mu_B$ per atom for Al. For the total moment a value of approximately $3\mu_B$ per formula unit is obtained, in agreement with the thumb rule for the magnetic moment μ of half-metallic Heusler alloys from $3d$-transition metals:[7] $\mu/\mu_B=N-24$, with N being the cumulated number of valence electrons ($4s$, $3d$ for the $3d$-transition metals and $3s$, $3p$ for Al). Experimentally determined magnetic moments for Co_2CrAl vary from $1.5\mu_B$ per formula unit to $3.0\mu_B$ per formula unit.[7]

Reproducible magnetic moments could be obtained in

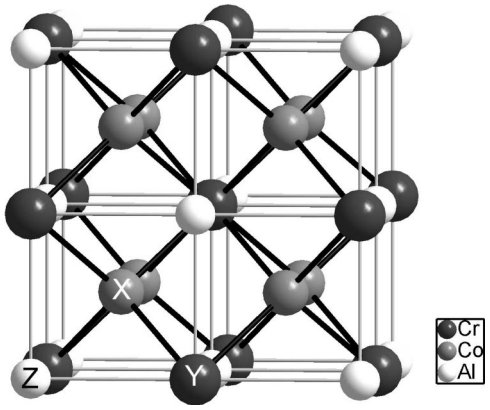

FIG. 1. Structure model of the Heusler alloy Co_2CrAl. In the Fe doped alloy $Co_2Cr_{0.6}Fe_{0.4}Al$ the Cr sites are partly occupied by the Fe atoms. The lattice constant $a=5.737$ Å for $Co_2Cr_{0.6}Fe_{0.4}Al$ was determined by the x-ray diffraction. The bonding distance between Co (tetrahedral site) and Cr (octahedral site) and between Co (tetrahedral site) and Al (octahedral site) is 2.48 Å, between two Co atoms and between Cr and Al 2.86 Å.

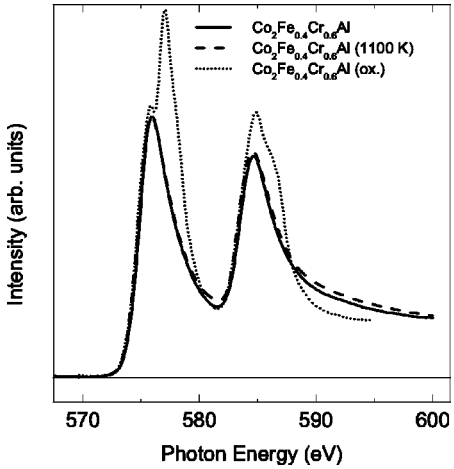

FIG. 2. Cr $2p\rightarrow 3d4s$ XAS spectra for Cr in $Co_2Cr_{0.6}Fe_{0.4}Al$. the XAS spectra for the quenched (solid line) and annealed (dashed line) sample measured after *in situ* cleaning of the surface are compared with the XAS spectra obtained for the quenched sample after exposure to air (dotted line). Prominent extra peaks at the L_{III} and L_{II} absorption edges for the exposed sample indicate oxidized Cr.

agreement with the thumb rule if Cr is partly replaced by Fe (Ref. 7). According to band structure calculations the electronic properties are mostly similar to Co_2CrAl. The replacement of Cr by Fe can be seen as a doping with electrons. For not properly prepared samples with a smaller magnetic moment than $3\mu_B$ per formula unit, Moessbauer spectroscopy revealed a nonmagnetic Fe component attributed to atomic disorder with Fe atoms occupying partly[7] Co (tetrahedral) sites. Band structure calculations for the disordered variant[7] confirm a strongly reduced magnetic moment ($1\mu_B$ per formula unit) as well as a loss of the half-metallic character.

In order to investigate element specific magnetic properties and compare them with theoretical predictions, we have carried out measurements of the magnetic circular dichroism (MCD) in the soft x-ray core-level absorption of the Cr, Fe, and Co $2p\rightarrow 3d$ excitation for $Co_2Cr_{0.6}Fe_{0.4}Al$.

II. EXPERIMENT

The ordered Heusler alloy $Co_2Cr_{0.6}Fe_{0.4}Al$ was prepared by the following method. First, the constituent elements were arc-melted under an argon atmosphere. Then, the samples were cooled down to room temperature by rapidly shutting down the heating (quenched samples). The obtained specimens were dense polycrystalline ingots.

Structural properties were measured by using x-ray diffraction as a standard method. The cubic structure (see Fig. 1) with a lattice constant of $a=5.737$ Å for $Co_2Cr_{0.6}Fe_{0.4}Al$ was confirmed for all specimens. Part of the samples were investigated by neutron diffraction revealing a small degree of atomic disorder for the quenched samples. For comparison a few samples were annealed at 1100 K for several days in vacuum. From the ingots we cut flat discs (8 mm diameter by 1 mm), which were then mechanically polished. Field dependent magnetic properties were measured by the superconducting quantum interference device (SQUID) magnetometry and by the magneto-optical Kerr effect (MOKE). Remanent magnetization was less than 10% of the saturation magnetization. Saturation was achieved for external fields larger than 0.2 T.

The MCD in Cr, Fe, and Co $2p\rightarrow 3d$ XAS (x-ray absorption spectroscopy) was measured at the undulator beamline U56/1-SGM at BESSY II (Berlin, Germany) and at the *First Dragon* beamline at the SRRC (Hsinchu, Taiwan). The resolution was set to about 80 meV at 800 eV. The XAS spectrum was obtained by the total electron yield method, measuring directly the sample current while scanning the photon energy. Absorption spectra were also taken by means of a fluorescence detector, for comparison. The sample current was normalized to the photon intensity measured via a gold mesh. It is assumed that the total yield of photoelectrons I^i is proportional to the absorption μ^i. The helicity of the light was fixed while two spectra with opposite directions of the external field, defined as μ^+ and μ^-, were acquired consecutively. The magnetic field applied to the sample (0.3 T) during the measurement was aligned with the surface normal and at an angle of 30° degrees with respect to the incident photon direction. Before the MCD measurement the surfaces were scraped *in situ* in ultrahigh vacuum in order to remove the surface oxide layer. The success of the scraping was confirmed by the vanishing of the O $1s$ absorption edge. All measurements were carried out at room temperature, i.e., lower than the Curie temperature of $Co_2Cr_{0.6}Fe_{0.4}Al$ ($T_C \approx 790$ K).

III. RESULTS AND DISCUSSION

A. Absorption spectra

Figures 2–4 show the averaged $2p\rightarrow 3d4s$ XAS spectra $\mu^+ + \mu^-$ for Cr, Fe, and Co in $Co_2Cr_{0.6}Fe_{0.4}Al$. These spectra consist of the L_{III} ($2p_{3/2}$) and L_{II} ($2p_{1/2}$) *white lines* split by the core hole's spin orbit interaction. The $2p\rightarrow 3d$ transition results in a resonant absorption line in addition to a

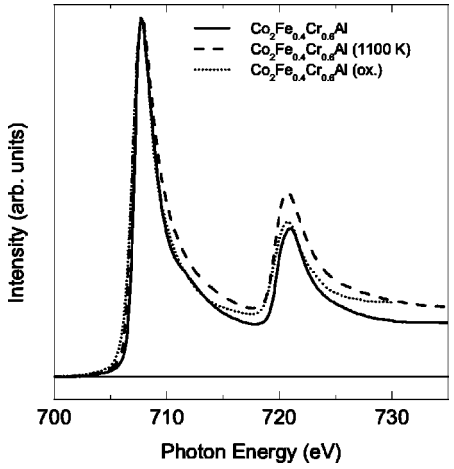

FIG. 3. Fe $2p \rightarrow 3d4s$ XAS spectra for Fe in $Co_2Cr_{0.6}Fe_{0.4}Al$. The XAS spectra for the quenched (solid line) and annealed (dashed line) sample measured after *in situ* cleaning of the surface are compared with the XAS spectra for the quenched sample after exposure to air (dotted line).

steplike increase of absorption due to $4s$ and $3d$ continuum partial densities of states (DOS), which are almost energy independent near the Fermi level. Spectra for the quenched specimen with a clean surface are compared with the spectra obtained for the same sample before removing the oxide layer and to a sample that has been annealed at 1100 K.

A clear difference is observed for the Cr XAS (see Fig. 2) before and after removing the oxide layer. For clean surfaces of both the quenched and the annealed sample, the XAS spectra look similar to spectra obtained from metallic Cr samples. Resonant absorption lines are obtained at 575.9 eV and 584.6 eV for L_{III} and L_{II} edges, respectively, with a full width at half maximum (FWHM) of ≈ 3.5 eV, which is characteristic for Cr in the metallic state.[20] Contrarily, the Cr XAS spectrum of the oxidized surface shows two distinct peaks at the L_{III} edge (575.9 eV and 577.0 eV) and the peak

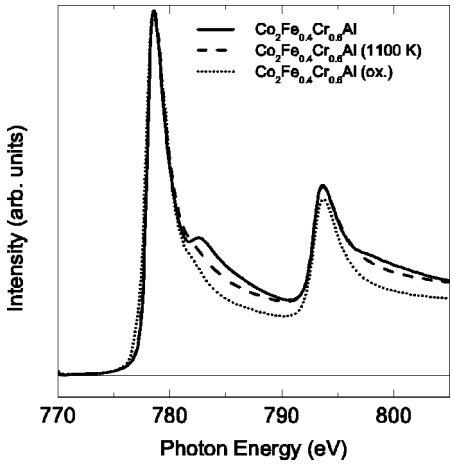

FIG. 4. Co $2p \rightarrow 3d4s$ XAS spectra for Co in $Co_2Cr_{0.6}Fe_{0.4}Al$. The XAS spectra for the quenched (solid line) and annealed (dashed line) sample measured after *in situ* cleaning of the surface are compared with the XAS spectra for the quenched sample after exposure to air (dotted line).

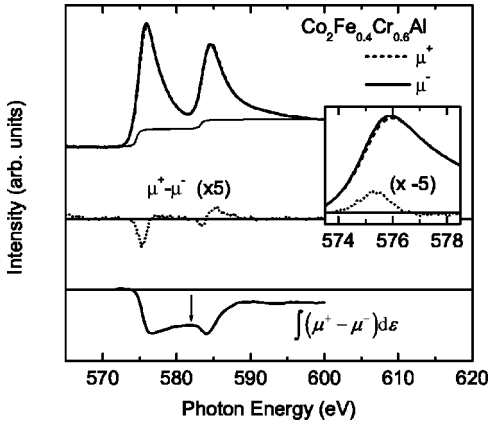

FIG. 5. Cr $2p \rightarrow 3d4s$ XAS-MCD spectra for Cr in the quenched $Co_2Cr_{0.6}Fe_{0.4}Al$ compound after *in situ* cleaning at 300 K. Solid (μ^-) and dashed (μ^+) lines show the XAS spectra measured with external field (0.3 T) applied parallel and antiparallel to the surface normal (oriented at an angle of 30° with respect to the photon spin). Dotted ($\mu^+ - \mu^-$) and solid [$\int(\mu^+ - \mu^-)d\varepsilon$] lines in the middle and bottom panels represent the MCD and its integrated spectra. The boundary between the L_{III} and L_{II} absorption regions is indicated by an arrow. The inset shows the expanded XAS-MCD spectra in the L_{III} region.

at the L_{II} edge is accompanied by a shoulder. The peak positions and relative intensities are characteristic for the XAS spectrum obtained from Cr_2O_3 (Ref. 21).

We approximate the steplike increase of intensity by the function

$$s = \frac{h}{3}\left[1 + \frac{2}{\pi}\arctan\left(\frac{\varepsilon - \varepsilon_3}{\Delta\varepsilon}\right)\right] + \frac{h}{6}\left[1 + \frac{2}{\pi}\arctan\left(\frac{\varepsilon - \varepsilon_1}{\Delta\varepsilon}\right)\right], \tag{1}$$

with $\Delta\varepsilon = 0.25$ eV denoting the energy broadening of the edges at ε_3 (for L_{III}) and ε_1 (for L_{II}) due to a combination of finite energy resolution, finite temperature, and lifetime broadening effects. The steplike function is shown, e.g., in Fig. 5.

If the radial matrix elements for the calculation of transition probabilities are supposed to be constant, the integrated XAS spectra $A_d = \int[\frac{1}{2}(\mu^+ + \mu^-) - s]d\varepsilon$ will provide a measure for the total number of d holes (neglecting hybridization), whereas the step height h is proportional to the DOS of s and continuum d states. Thus, the value $q_d = A_d/h$ denotes a measure for the relative contribution of transitions into localized d states to the absorption spectra. For the quenched and the annealed samples we obtain almost identical values $q_d = 27.6$ eV and $q_d = 28.3$ eV, whereas the oxidized surfaces show a larger value $q_d = 36.8$ eV. This observation indicates an increase of d holes on the expense of s holes, which is characteristic for an electron transfer depletion due to oxidation.

Figure 3 shows the XAS spectra at the Fe $L_{II,III}$ edge for the same set of samples. For all three cases the spectra show the resonant absorption lines at 707.7 eV and 721 eV for the L_{III} and L_{II} edge, respectively, with a FWHM of ≈ 2 eV, similar to the XAS spectra of metallic Fe (Ref. 22). In par-

ticular, the oxidized sample does not show an additional peak at the L_{III} edge, which could be expected at a photon energy shifted by 2 eV to higher binding energy.[23] A weak shoulder at the L_{III} edge at 712 eV ($\Delta\varepsilon \approx 4$ eV) can be recognized for the quenched sample, which is absent for the annealed and the oxidized sample. The relative contribution of transitions into *d* holes to the absorption spectra is largest for the quenched sample ($q_d = 27.3$ eV) and becomes smaller after annealing ($q_d = 24.9$ eV) or oxidizing ($q_d = 22.5$ eV). For metallic Fe a value of $q_d = 25$ eV was reported.[22]

As in the case of Fe, the XAS spectra at the Co $L_{II,III}$ edge (Fig. 4) shows two prominent resonant peaks corresponding to the L_{III} and L_{II} component at 778.6 eV and 793.8 eV, similar to the XAS spectra observed for metallic Co (Ref. 22). The FWHM is approximately 2 eV. No additional peaks can be recognized for the oxidized sample. In particular, no many-peak structures in the L_{III} region were observed as in the case of the Sn-based Heusler alloys Co_2YSn (Y = Ti, Zr, and Nb).[16] The lack of these many-peak structures cannot be attributed to a limited energy resolution as can be concluded from the steep increase at 778 eV. Instead it must be explained by a different DOS that indicates a more metallic character of the Co *d* band compared to the Co_2YSn alloys. For the quenched sample we observed a pronounced shoulder at the L_{III} peak shifted by 4 eV with respect to the maximum to a higher photon energy. A similar structure should be observed in the L_{II} region. A less pronounced shoulder can indeed be observed at the L_{II} peak. Less sharp structures in the L_{II} region can be ascribed to a lifetime broadening effect because the lifetime of the $2p_{1/2}$ core hole is much shorter than the $2p_{3/2}$ core hole due to the Coster-Kronig decay.[16]

In contrast to the Fe XAS, the relative contribution of transitions into Co *d* holes to the absorption spectra increases after oxidation. For the quenched (annealed) sample we obtained a value of $q_d = 15.8$ eV (15.6 eV), whereas oxidized samples show values $q_d = 17.5$–19.5 eV. For metallic Co a value of $q_d = 21$ eV was reported.[22]

From the comparison of the XAS spectra of oxidized samples with clean surfaces it is obvious that the three elements Cr, Fe, and Co react differently when exposed to air. This can be expected, because the metal-oxygen bond enthalpy is larger for Cr (430 kJ/mol) than for Fe (400 kJ/mol) and Co (385 kJ/mol). The strong selectivity, however, is surprising. Cr is selectively oxidized, whereas the majority of Co and Fe remains in a metallic state. The information depth of the XAS involves a surface layer of 1–2 nm thickness, i.e., 2–4 unit cells. Therefore, the selective oxidation of Cr involves a surface segregation process, which at least partially destroys the stoichiometry of the Heusler alloy in the surface region. This is supported by the observation that the relative number of *d* holes increases in the case of Co and decreases in the case of Fe upon oxidation. In both cases q_d approaches the corresponding bulk value. Taking this into account, one may conclude that the near surface region of about 1–2 nm consists of metallic FeCo alloy mixed by Cr oxide, after exposure to air. From its chemical reactivity (Al—O bond enthalpy 511 kJ/mol) one might assume that Al is oxidized as well.

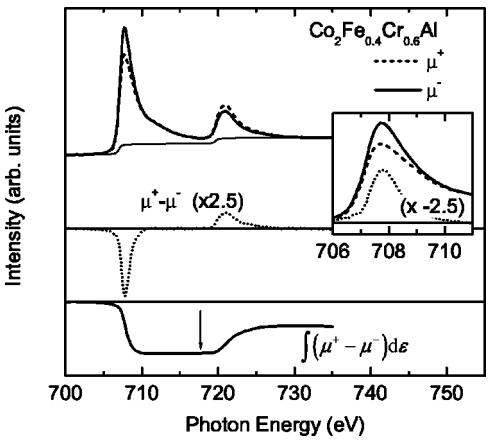

FIG. 6. Fe $2p \rightarrow 3d4s$ XAS-MCD spectra for Fe in the quenched $Co_2Cr_{0.6}Fe_{0.4}Al$ compound after *in situ* cleaning at 300 K. Same conditions and notations as in Fig. 5.

B. Magnetic circular dichroism

In Figures 5–7 are plotted the $2p \rightarrow 3d4s$ XAS spectra μ^+ and μ^- and the corresponding MCD spectra $\mu^+ - \mu^-$ for Cr, Fe, and Co in the quenched $Co_2Cr_{0.6}Fe_{0.4}Al$ sample. The MCD spectra are expanded (factor 2.5 and 5) in order to make the spectral features visible. The lower panels show the integrated MCD spectra. Negative peaks in the MCD spectra are seen in the L_{III} region and much smaller positive peaks in the L_{II} region for all three elements. This indicates that the total magnetic moment is dominated by the spin contribution. The orbital contribution is small but parallel to the spin moment.

For the case of Cr (see Fig. 5), the maxima of μ^+ and μ^- do not coincide. Therefore, one obtains a characteristic change of sign of the MCD near the absorption maximum. This feature has been predicted from atomic calculations.[24] For Fe/Cr multilayers, in which Cr was polarized, a similar feature has been observed experimentally for Cr in the metallic state.[20] The MCD spectra of Fe and Co show maxima at the same energy position as the maximum of the absorption. Both the MCD spectra (see Figs. 6 and 7) look similar to the spectra observed for bulk metallic systems.[22]

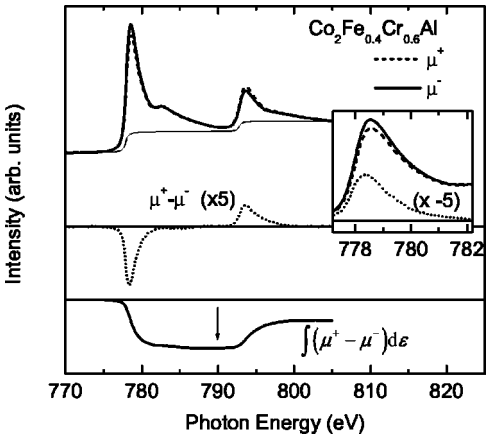

FIG. 7. Co $2p \rightarrow 3d4s$ XAS-MCD spectra for Co in the quenched $Co_2Cr_{0.6}Fe_{0.4}Al$ compound after *in situ* cleaning at 300 K. Same conditions and notations as in Fig. 5.

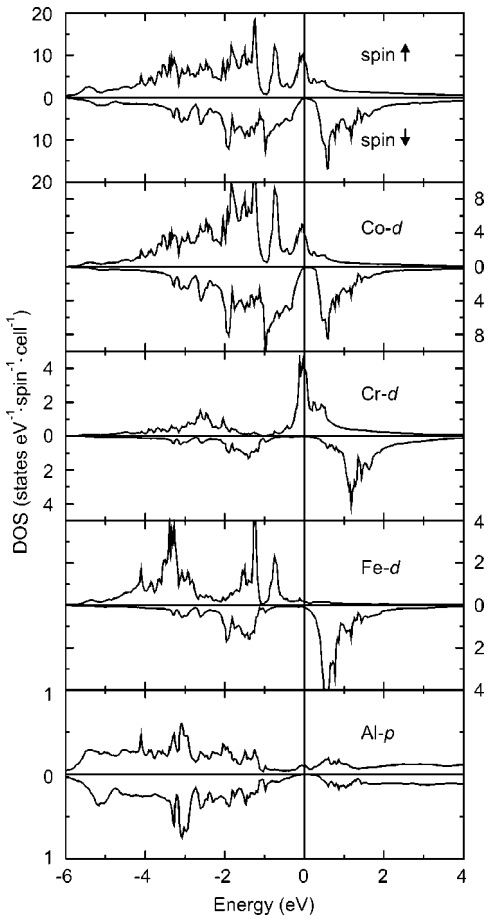

FIG. 8. Co, Fe, Cr, and Al partial DOS of the ferromagnetic Heusler alloy $Co_2Cr_{0.5}Fe_{0.5}Al$ (Ref. 7). The electronic structures are computed by the tight-binding linear muffin-tin orbital atomic-sphere approximation (LMTO-ASA) method for a $L2_1$ cubic structure with every second Cr atom replaced by Fe. Wigner-Seitz radii were chosen for the muffin-tin radii and for the calculation of magnetic moments. The Fermi level is marked by a solid line at $\varepsilon = 0$ eV.

We did not recognize the complex atomic multiplet structure in the XAS as well as in the MCD, which were obtained from the atomic calculations.[24] An alternative model is provided by the band structure calculations. In the single-electron picture, the $2p \rightarrow 3d$ transitions reflect the unoccupied part of the $3d$ partial density of states (PDOS). The prominent feature in the $3d$ PDOS is a narrow peak in the minority band 0.5 eV (for Co and Fe) and 1.0 eV (for Cr) above the Fermi level (see Fig. 8). For the majority band the $3d$ PDOS shows a smaller maximum value directly at the Fermi level for Co and Cr. Hence, one would expect a shift of the absorption maximum to higher photon energies for the transition into the minority band (positive magnetization) with respect to the transition into the unoccupied part of the majority band (negative magnetization). Our experiment instead shows a shift to smaller photon energy (for Cr, Fig. 5) or no shift (for Fe and Co, Figs. 6 and 7). Only the Cr L_{II} signal around 585 eV in Fig. 5 shows the anticipated behavior in accordance with the Cr majority and minority PDOS features above the Fermi level (cf. Fig. 8). Thus, the single-electron model is not sufficient in order to explain the experimentally obtained spectra and one has to consider a strong interaction between the $2p$ core hole and the $3d$ and $4s$ electrons in the final state.

C. Sum rule analysis

In order to quantitatively discuss spin μ_s and orbital μ_l momenta contribution to the magnetic moment, we apply the magneto-optical sum rules, as discussed in Refs. 25 and 26, neglecting the magnetic dipole operator as proposed, i.e., in Ref. 27:

$$\mu_s = -\frac{N_h}{P\cos\theta}\frac{A_{3/2}-2A_{1/2}}{A_d}\mu_B, \tag{2}$$

$$\mu_l = -\frac{2N_h}{3P\cos\theta}\frac{A_{3/2}+A_{1/2}}{A_d}\mu_B, \tag{3}$$

with $A_j = \int_j (\mu^+ - \mu^-) d\varepsilon$ being the integrated MCD spectra at the L_{III} ($j=3/2$) and L_{II} ($j=1/2$) edges. The boundary between the L_{III} and L_{II} edges was set to the minimum of the absorption spectra between the two peaks. A_d denotes the integrated XAS spectra into d states as discussed above. The polarization was estimated $P=0.8$ and the photon incident angle is $\theta = 30°$ with respect to the magnetic field direction. The number of d holes N_h is different for the three elements Cr, Fe, and Co, and in metallic systems it differs slightly from the corresponding atomic values. N_h cannot be determined quantitatively from the XAS spectra. It is difficult to determine N_h precisely for an unknown compound, although it is essential for the calculation of magnetic moments [Eq. 3)]. Even for pure elements varying values have been given, i.e., $2.43 < N_h(\mathrm{Co}) < 2.8$ (Refs. 22, 28, and 29). For Co and Fe we have chosen most likely values, as determined for the metallic systems,[22] $N_h(\mathrm{Co}) = 2.49$ and $N_h(\mathrm{Fe}) = 3.39$, by calibration with bulk magnetization. This is not possible for Cr. Instead, we set $N_h(\mathrm{Cr}) = 6$ to the atomic ground-state value. These values are in agreement (within an error of 10%) with the theoretical calculations discussed below.

While the error due to data fluctuations is negligible, an experimental error of 10% for the determination of magnetic moments is due to the error of P and to the background subtraction. An additional error of the same order of magnitude arises from the uncertainty of N_h, which only affects absolute values, and from the intermixing between the L_{II} and L_{III} edge, which mainly affects the ratio of spin and orbital moments particularly for Cr. Moreover, the magnetic dipole operator cannot be neglected for strongly correlated electronic systems, Heusler alloys being on the borderline. Because the latter systematic errors cannot be quantified easily, they are not included in the error margins given below. We anticipate that the total error is less than 25%.

Results for the three samples are summarized in Table I. For the quenched alloy we observe a finite magnetic moment per Cr atom of $\mu(\mathrm{Cr}) = \mu_s + \mu_l = 0.17(2)\mu_B$. For Co and Fe we obtain $\mu(\mathrm{Co}) = 0.41(4)\mu_B$ and $\mu(\mathrm{Fe}) = 1.03(10)\mu_B$. The magnetic moment per formula unit results in $\mu_{\mathrm{sum}} = 1.3(2)\mu_B$, which is considerably smaller than the magne-

TABLE I. Element specific properties for Cr, Fe, and Co in $Co_2Cr_{0.6}Fe_{0.4}Al$. Results for a quenched (a), annealed (b), and the quenched sample after exposure to air (c) are shown. The ratio $q_d = A_d/h$ denotes a measure for the relative contribution of transitions into *d* states to the absorption spectra (see text). Using the sum rules, we obtained values for the element specific polarization $\mu/N_h = (\mu_s + \mu_l)/N_h$ and the magnetic moments $\mu = \mu_s + \mu_l$ per atom. The specific number of *d* holes were set to $N_h(\mathrm{Co}) = 2.49$, $N_h(\mathrm{Fe}) = 3.39$, and $N_h(\mathrm{Cr}) = 6$. The summarized magnetic moment per formula unit $\mu_{\mathrm{sum}} = 2\mu(\mathrm{Co}) + 0.6\mu(\mathrm{Cr}) + 0.4\mu(\mathrm{Fe})$ is compared with the magnetic moment per formula unit measured by the SQUID magnetometry at 300 K.

		q_d (eV)	$\mu_s+\mu_l$ ($N_h\mu_B$)	$\mu_s+\mu_l$ (μ_B)	μ_{sum} (μ_B/formula unit)	μ (300 K) (μ_B/formula unit)
(a) Quenched	Cr	27.6	0.028	0.168		
	Fe	27.3	0.305	1.034	1.34	3.2
	Co	15.8	0.166	0.413		
(b) Annealed	Cr	28.3	<0.005	<0.03		
	Fe	24.9	0.093	0.315	0.55	1.7
	Co	15.6	0.086	0.214		
(c) Oxidized	Cr	36.8	<0.005	<0.03		
	Fe	22.0	0.516	1.75	2.86	3.2
	Co	18.0	0.434	1.08		

tization determined by magnetometry ($3.2\mu_B$). A lack of magnetization was found for the annealed sample, too. Contrarily, the oxidized sample shows a summarized magnetic moment of $\mu_{\mathrm{sum}} = 2.9(3)\mu_B$ per formula unit, close to the magnetometrically determined value. For some annealed samples (not shown here) the magnetic moment determined by the MCD-XAS even exceeds the bulk moment. This observation supports the selective oxidation scenario discussed above. The oxidized Cr has lost its magnetic moment, whereas the magnetic moments of Co and Fe atoms approach their metallic bulk moments.

Comparatively small magnetic moments were observed for all samples with clean surfaces after the *in situ* scraping. This may originate from the situation that the magnetic field is not high enough to saturate the magnetization at the scraped surface, particularly in the rough surface region, where mechanical stress and dislocations provoke closure domains. Alternatively, a reduced magnetization at the free surface could be an inherent property of $Co_2Cr_{1-x}Fe_xAl$.

For the following discussion we assume that the magnetization is reduced by a common factor for the constituents of the compound. Absolute values of the magnetic moments can be estimated, using the values of the total magnetic moment per formula unit obtained by a magnetization measurement at saturation. In order to compare with theoretical moments in the ground state we used magnetization values extrapolated to 0 K from the temperature-dependent magnetization measurements at 4 K$<T<$300 K. Because the magnetic moments of Cr, Fe, and Co are dominant in the compound we neglect the contribution of Al. The band structure calculations predict a moment of only $-0.1\mu_B$ for Al, antiparallel to the main magnetization direction. By using the ratio μ_l/μ_s determined from the MCD, we have obtained the values for the spin μ_s and orbital μ_l magnetic moments,

TABLE II. Ratio of the orbital magnetic moment to the spin magnetic moment for Cr, Fe, and Co atoms, respectively, in $Co_2Cr_{0.6}Fe_{0.4}Al$. Results for the quenched (a) and annealed (b) compounds are compared. Magnetic moments μ (0 K) per formula unit, extrapolated from the SQUID magnetometry, were used to obtain element specific magnetic ground-state moments $\mu_{\mathrm{sum}} = \mu_s + \mu_l$ per atom from the MCD (see Table I), assuming a common calibration factor for each sample. Theoretical results $\mu_{s,\mathrm{band}}$ from band structure calculations (Ref. 7) are given for comparison.

		μ_l/μ_s	μ (0 K) (μ_B/formula unit)	μ_{sum} (μ_B)	μ_s (μ_B)	μ_l (μ_B)	$\mu_{s,\mathrm{band}}$ (μ_B)
(a) Quenched	Cr	0.10		0.44	0.40	0.04	1.52
	Fe	0.14	3.5	2.70	2.37	0.33	2.77
	Co	0.13		1.08	0.96	0.12	0.96
(b) Annealed	Cr			<0.03			
	Fe	0.20	1.9	1.09	0.90	0.19	
	Co	0.14		0.74	0.65	0.09	

separately, as shown in Table II. For the quenched samples, Fe has the largest magnetic moment per atom, while Co and Cr moments are much smaller. Within error limits, the annealing procedure suppresses completely the contribution of the Cr atoms to the total magnetic moment. The magnetic moment of Fe atoms is reduced to a large extent ($1.1\mu_B$ instead of $2.7\mu_B$ for the quenched sample).

The latter observation confirms previous investigations by Moessbauer spectroscopy,[7] revealing a paramagnetic component in the hyperfine field spectra after annealing. The paramagnetic component was interpreted as Fe atoms occupying tetrahedral (Co) sites, whereas in quenched samples Fe occupies only octahedral sites. The spin magnetic moments μ_s can be compared with the band structure calculations shown in Fig. 8. In the calculation, spin-orbit coupling is not taken into account and therefore no orbital magnetic moment is present. For the quenched (and well-ordered) sample spin magnetic moments of Co ($0.96\mu_B$ per atom) and Fe ($2.37\mu_B$ per atom) are reproduced by the calculations ($0.96\mu_B$ and $2.77\mu_B$ per atom). The moment of Cr atoms ($0.40\mu_B$ per atom) is considerably smaller than predicted by theory ($1.52\mu_B$ per atom). Hence, the missing magnetic moment comparing the total spin moment ($3.1\mu_B$ per formula unit) of the quenched sample with the prediction from the band structure calculation ($3.8\mu_B$ per formula unit) is mainly due to a reduction of the Cr moment. On the experimental part, the origin of the prominent decrease might be a remaining disorder with Cr atoms occupying tetrahedral sites similar to the Fe atoms in annealed samples. However, neutron diffraction data could be nicely refined with the assumption of an ordered sample.[7] Considering the theoretical calculations, the LMTO method might be a too crude approximation. However, for the Heusler alloy Co_2TiSn similar calculations nicely fits the experiment.[16] An alternative explanation could be an antiferromagnetic orientation of neighboring Cr atoms in the fcc structure, similar to a NiO magnetic structure.

The orbital magnetic moment of $3d$ elements in cubic lattices[30] is usually small compared to the spin moment. However, it is of great relevance because it determines the magnitude of the magnetic anisotropy.[31] For the quenched sample we observe a ratio $\mu_l/\mu_s = 0.13(2)$ for Co atoms, which is close to the values reported for metallic alloys, whereas Fe atoms possess a large orbital moment $\mu_l/\mu_s = 0.14(2)$ in comparison with bulk values. According to a discussion based on the second-order perturbation theory, the orbital magnetic moment of a Heusler alloy arises from the mixing either in the t_{2g} orbitals or between t_{2g} and e_g orbitals. A large magnetic anisotropy could be expected in these alloys. After annealing, μ_l/μ_s is not changed for Co but increases for Fe. This could be the result of lattice distortion due to the increased disorder.

IV. SUMMARY

We have measured the MCD in the Cr, Fe, and Co $2p \rightarrow 3d4s$ XAS of the ferromagnetic Heusler alloy $Co_2Cr_{0.6}Fe_{0.4}Al$. We observed a strong selective oxidation of Cr when polished surfaces are exposed to air, involving a change of electronic properties at the surface. The differing properties of the surface compared to the bulk have to be taken into account for the interpretation of magnetoresistance effects in powder compacts[32,33] and of Andreev reflections[34] with respect to a potentially high spin-polarization of the Heusler alloys. It is, in particular, important for the observed significant decrease of the magnetoresistance in pressed Heusler alloy powders[7] or the possibility to verify a total spin polarization by means of Andreev reflections, using the HMF Heusler alloys.[35] A selective oxidation at the surface could potentially lead to a misinterpretation of the results, using the latter method.

We have evaluated element specific magnetic moments by magneto-optical sum rules. Absolute values of spin and orbital magnetic moments were estimated by using values of the total magnetic moment obtained by the SQUID magnetometry. For quenched samples we obtained spin magnetic moments in agreement with the band structure calculations for Co and Fe atoms, whereas Cr atoms possess a reduced magnetic moment. Orbital magnetic moments are 10% (13%) of the spin moment for Cr (Co). For Fe the orbital moment is 14% of the spin moment, corresponding to the absolute value of $0.33\mu_B$, which is considerably larger than the Fe bulk value [$0.09\mu_B$ (Ref. 22)]. We attribute the origin of the large orbital moment of Fe to the localization of the Fe $3d$ electrons. Annealing of $Co_2Cr_{0.6}Fe_{0.4}Al$ reduces magnetic moments at Fe and Cr atoms drastically, which we tentatively attribute to increased atomic disorder. Atomic disorder seems to play a major role for the magnetic properties of Heusler alloys. Element specific magnetometry in combination with the theoretical band structure calculations provides a key tool to the understanding of the influence of disorder and of the particular electronic properties of the Heusler alloys.

ACKNOWLEDGMENTS

The authors thank all members of BESSY II (Berlin, Germany) and SRRC (Hsinchu, Taiwan) for their help during the beamtimes. G.H.F. and S.W. are very grateful to Y. Hwu (Academia Sinica, Taipei) and H.-M. Lin (Tatung University, Taipei) for their support during the experiments in Taiwan.

[1] G.A. Prinz, Science **282**, 1660 (1998).
[2] R.A. de Groot, F.M. Mueller, P.G. van Engen, and K.H.J. Buschow, Phys. Rev. Lett. **50**, 2024 (1983).
[3] S.J. Youn and B.I. Min, Phys. Rev. B **51**, 10436 (1995).
[4] D. Ristoiu, J.P. Nozières, C.N. Borca, T. Komesu, H.-K. Jeong, and P.A. Dowben, Europhys. Lett. **49**, 624 (2000).
[5] W. Zhu, B. Sinkovic, E. Vescovo, C. Tanaka, and J.S. Moodera, Phys. Rev. B **64**, 060403 (2001).

[6] S. Plogmann, T. Schlathölter, J. Braun, M. Neumann, Yu M. Yarmoshenko, M. Yablonskikh, E.I. Shreder, E.Z. Kurmaev, A. Wrona, and A. Slebarski, Phys. Rev. B **60**, 6428 (1999).
[7] T. Block, C. Felser, G. Jakob, J. Ensling, B. Mühling, P. Gütlich, and R. J. Cava (unpublished).
[8] P.J. Webster and K.R.A. Ziebeck, J. Phys. Chem. Solids **34**, 1647 (1973).
[9] M. Terada, Y. Fujita, and K. Endo, J. Phys. Soc. Jpn. **36**, 620 (1974).
[10] K. Endo, K. Ooiwa, and A. Shinogi, J. Magn. Magn. Mater. **104-107**, 2014 (1992).
[11] K.R.A. Ziebeck and P.J. Webster, J. Phys. Chem. Solids **35**, 1 (1974).
[12] P.G. van Engen, K.H.J. Buschow, and M. Erman, J. Magn. Magn. Mater. **30**, 374 (1983).
[13] M.V. Yablonskikh, Yu. M. Yarmoshenko, V.I. Grebennikov, E.Z. Kurmaev, S.M. Butorin, L.-C. Duda, J. Nordgren, S. Plogmann, and M. Neumann, Phys. Rev. B **63**, 235117 (2001).
[14] S. Ishida, S. Akazawa, Y. Kubo, and J. Ishida, J. Phys. F: Met. Phys. **12**, 1111 (1982).
[15] A. Jezierski, Phys. Status Solidi B **196**, 357 (1996).
[16] A. Yamasaki, S. Imada, R. Arai, H. Utsunomiya, S. Suga, T. Muro, Y. Saitoh, T. Kanomata, and S. Ishida, Phys. Rev. B **65**, 104410 (2002).
[17] K.H.J. Buschow and P.G. van Engen, J. Magn. Magn. Mater. **25**, 90 (1981).
[18] A. Slebarski, M. Neumann, and B. Schneider, J. Phys.: Condens. Matter **13**, 5515 (2001).
[19] S. Wurmehl, Diploma thesis, Johannes Gutenberg-University Mainz, 2002; Thomas Block, Ph.D. thesis, Johannes Gutenberg-University Mainz, 2002.
[20] M.A. Tomaz, W.J. Antel, W.L. O'Brien, and G.R. Harp, Phys. Rev. B **55**, 3716 (1997).
[21] C. Theil, J. van Elp, and F. Folkmann, Phys. Rev. B **59**, 7931 (1999).
[22] C.T. Chen, Y.U. Idzerda, H.-J. Lin, N.V. Smith, G. Meigs, E. Chaban, G.H. Ho, E. Pellegrin, and F. Sette, Phys. Rev. Lett. **75**, 152 (1995).
[23] J.F. Hochepied, Ph. Sainctavit, and M.P. Pileni, J. Magn. Magn. Mater. **231**, 315 (2001).
[24] G. van der Laan and B.T. Thole, Phys. Rev. B **43**, 13 401 (1991).
[25] B.T. Thole, P. Carra, F. Sette, and G. van der Laan, Phys. Rev. Lett. **68**, 1943 (1992).
[26] P. Carra, B.T. Thole, M. Altarelli, and X. Wang, Phys. Rev. Lett. **70**, 694 (1993).
[27] S. Imada, T. Muro, T. Shishidou, S. Suga, H. Maruyama, K. Kobayashi, H. Yamazaki, and T. Kanomata, Phys. Rev. B **59**, 8752 (1999).
[28] G.Y. Guo, H. Ebert, W.M. Temmerman, and P.J. Durham, Phys. Rev. B **50**, 3861 (1994).
[29] P. Söderlind, O. Eriksson, B. Johansson, R.C. Albers, and A.M. Boring, Phys. Rev. B **45**, 12 911 (1992).
[30] S. Ishida, Y. Otsuka, Y. Kubo, and J. Ishida, J. Phys. F: Met. Phys. **13**, 1173 (1983).
[31] J. Stöhr, J. Magn. Magn. Mater. **200**, 470 (1999).
[32] A. Gupta and J.Z. Sun, J. Magn. Magn. Mater. **200**, 24 (1999).
[33] J.M.D. Coey, A.E. Berkowitz, Ll. Balcells, F.F. Putris, and A. Barry, Phys. Rev. Lett. **80**, 3815 (1998).
[34] R.J. Soulen, Jr., J.M. Byers, M.S. Osofsky, B. Nadgorny, T. Ambrose, S.F. Cheng, P.R. Broussard, C.T. Tanaka, J. Nowak, J.S. Moodera, A. Barry, and J.M.D. Coey, Science **282**, 85 (1998).
[35] N. Auth, G. Jakob, T. Block, and C. Felser (unpublished).